Phonon- and phason-type spherical inclusions in icosahedral quasicrystals

2003 J. Phys.: Condens. Matter 15 L363

(http://iopscience.iop.org/0953-8984/15/24/102)

INSTITUTE OF PHYSICS PUBLISHING JOURNAL OF PHYSICS: CONDENSED MATTER

J. Phys.: Condens. Matter **15** (2003) L363–L370 PII: S0953-8984(03)62509-9

LETTER TO THE EDITOR

Phonon- and phason-type spherical inclusions in icosahedral quasicrystals

Jianbo Wang[1,2,3,5], **L Mancini**[4], **Renhui Wang**[1,2] **and J Gastaldi**[3]

[1] Department of Physics, Wuhan University, Wuhan 430072, People's Republic of China
[2] Centre for Electron Microscopy, Wuhan University, Wuhan 430072, People's Republic of China
[3] CRMC2-CNRS, Campus de Luminy, case 913, 13288 Marseille Cedex 09, France
[4] SYRMEP Group, Sincrotrone Trieste SCpA, 34012 Basovizza (Trieste), Italy

E-mail: wang@whu.edu.cn

Received 23 April 2003
Published 6 June 2003
Online at stacks.iop.org/JPhysCM/15/L363

Abstract

Analytical expressions are derived as a first-order approximation for the elastic displacement fields, including both phonon- and phason-type components, induced by spherical inclusions in icosahedral quasicrystals (IQCs). The phonon-type component obtained is the same as that for a spherical inclusion in conventional elastically isotropic crystals, while the expression for the phason-type displacement, which decreases with increasing distance r to the sphere centre as r^{-1}, is derived for the first time. Three concrete cases are discussed. The phonon part of the analytical expressions has been used to simulate the black–white double-lobe contrasts in the x-ray topograph (XRT) images of the strain field around the pores in the AlPdMn IQCs. The analytical expression for the phason-type displacement is used to simulate the XRT images of the strain field around spherical inclusions having isomorphic structures. The striking resemblance between experimental and simulated images suggests that such inclusions are surrounded by antiphase boundaries with a phason-type displacement vector, being particular structural defects in IQCs.

1. Introduction

Icosahedral quasicrystals (IQCs) can be described as a three-dimensional (3D) cut of a six-dimensional (6D) hypercubic crystal [1]. A 6D hyperspace may be divided into two 3D subspaces, the parallel or physical space $E^{\parallel}$ and the perpendicular or mathematical space $E^{\perp}$. Consequently, the displacement field around a defect in quasicrystals consists of two components, $\boldsymbol{u}$ and $\boldsymbol{w}$. The phonon-type displacement field $\boldsymbol{u} \in E^{\parallel}$ is analogous to the field in conventional crystals. The phason-type displacement field $\boldsymbol{w} \in E^{\perp}$ is peculiar to quasicrystals.

[5] Author to whom any correspondence should be addressed.

There are two cases to be discussed here. First, when two domains of an IQC are obtained by cutting a same 6D hypercubic crystal at different distances from the origin along the perpendicular direction, these two domains are in the same local isomorphism class but with a constant phason-type displacement $\boldsymbol{w}$. As pointed out by Levine and Steinhardt [2] and Socolar and Steinhardt [3], two quasicrystals are in the same local isomorphism class if and only if (1) every finite atomic configuration in each occurs in the other; and (2) they have diffraction patterns with identical intensities. Second, when the phason-type displacement $\boldsymbol{w}(\boldsymbol{r})$ is a function of the position vector $\boldsymbol{r}$, the varying phason-type displacement will cause some atom, which contributes an atom at the position A of the quasicrystal, in the high-dimensional crystal to be shifted out of the physical space, and hence the atom A in the physical space disappears. At the same time some other nearby atom in the high-dimensional crystal is shifted into the physical space, and hence contributes to an atom at the position B in the physical space. This is equivalent to saying that the phason-type displacement causes the atom at the position A to flip to the position B. Recently, Edagawa *et al* [4] observed directly the flips of atomic columns in decagonal Al–Cu–Co quasicrystals by high-resolution transmission electron microscopy. Both phonon- and phason-type defects have a strong influence on the mechanical and physical properties of quasicrystal materials [1].

Considering this peculiarity of quasicrystals in which there are phason-type displacements in addition to the conventional phonon-type displacements, the elasticity theory was generalized to the case of quasicrystals (for example, [5–9]). Furthermore, the generalized elasticity theory was successfully used to calculate the displacement fields around dislocation lines in various quasicrystals (for example, [5–8] and papers cited therein). However, as far as spherical inclusions are concerned, there has never been an attempt to generalize the classic expression for the displacement field in an elastically isotropic crystal [10] to the case of quasicrystals. This lack of theoretical consideration is in sharp contrast to the tremendous quantity of experimental results [11–24], which is probably due to the spherical inclusions in IQCs.

The purpose of the present letter is to derive analytical expressions for both the phonon-type and phason-type displacement fields, induced by a spherical inclusion in an IQC, with some simplifications. These results are discussed in three cases for studying spherical defects in IQCs, such as antiphase domains and pores (holes). Further probable concrete characterization is considered for some experimental results [11–24].

2. Deducing an analytical expression for the elastic displacement field

According to the generalized elasticity theory, the displacement field variables $\boldsymbol{u}$ and $\boldsymbol{w}$ for IQCs must satisfy the basic elasticity equilibrium equation in the Cartesian coordinate system, with $\boldsymbol{e}_i$ and $\boldsymbol{e}_i^{\perp}$ $(i = 1, 2, 3)$ the basis unit vectors in the parallel and perpendicular subspaces, respectively, adopted by Ding *et al* as follows [5, 6, 9]:

$$\begin{aligned}
&\mu\nabla^2 u_1 + (\lambda+\mu)\partial_1(\boldsymbol{\nabla}\cdot\boldsymbol{u}) + R(\partial_1\partial_1 w_1 + 2\partial_1\partial_3 w_1 - \partial_2\partial_2 w_1 \\
&\qquad + 2\partial_1\partial_2 w_2 - 2\partial_2\partial_3 w_2 + 2\partial_1\partial_3 w_3) + f_1 = 0, \\
&\mu\nabla^2 u_2 + (\lambda+\mu)\partial_2(\boldsymbol{\nabla}\cdot\boldsymbol{u}) + R(-2\partial_1\partial_2 w_1 - 2\partial_2\partial_3 w_1 + \partial_1\partial_1 w_2 \\
&\qquad - 2\partial_1\partial_3 w_2 - \partial_2\partial_2 w_2 + 2\partial_2\partial_3 w_3) + f_2 = 0, \\
&\mu\nabla^2 u_3 + (\lambda+\mu)\partial_3(\boldsymbol{\nabla}\cdot\boldsymbol{u}) + R(\partial_1\partial_1 w_1 - \partial_2\partial_2 w_1 \\
&\qquad - 2\partial_1\partial_2 w_2 + \partial_1\partial_1 w_3 + \partial_2\partial_2 w_3 - 2\partial_3\partial_3 w_3) + f_3 = 0, \\
&K_1\nabla^2 w_1 + K_2(2\partial_1\partial_3 w_1 - \partial_3\partial_3 w_1 + 2\partial_2\partial_3 w_2 + \partial_1\partial_1 w_3 - \partial_2\partial_2 w_3) \\
&\qquad + R(\partial_1\partial_1 u_1 - \partial_2\partial_2 u_1 + 2\partial_1\partial_3 u_1 - 2\partial_1\partial_2 u_2 - 2\partial_2\partial_3 u_2 + \partial_1\partial_1 u_3 - \partial_2\partial_2 u_3) \\
&\qquad + g_1 = 0,
\end{aligned} \tag{1}$$

$$K_1\nabla^2 w_2 + K_2(2\partial_2\partial_3 w_1 - 2\partial_1\partial_3 w_2 - 2\partial_1\partial_2 w_3 - \partial_3\partial_3 w_2) + R(2\partial_1\partial_2 u_1 - 2\partial_2\partial_3 u_1 + \partial_1\partial_1 u_2 - \partial_2\partial_2 u_2 - 2\partial_1\partial_3 u_2 - 2\partial_1\partial_2 u_3) + g_2 = 0,$$
$$(K_1 - K_2)\nabla^2 w_3 + K_2(\partial_1\partial_1 w_1 - \partial_2\partial_2 w_1 - 2\partial_1\partial_2 w_2 + 2\partial_3\partial_3 w_3) + R(2\partial_1\partial_3 u_1 + 2\partial_2\partial_3 u_2 + \partial_1\partial_1 u_3 + \partial_2\partial_2 u_3 - 2\partial_3\partial_3 u_3) + g_3 = 0,$$

where $\boldsymbol{u} = \sum_{i=1}^{3} u_i \boldsymbol{e}_i$, $\boldsymbol{w} = \sum_{i=1}^{3} w_i \boldsymbol{e}_i^{\perp}$; λ, μ, R, K_1 and K_2 are five independent elastic constants for IQCs, in which λ and μ are related to the phonons, K_1, K_2 to the phasons, R to the phonon–phason coupling; and $\boldsymbol{f} = \sum_{i=1}^{3} f_i \boldsymbol{e}_i$, $\boldsymbol{g} = \sum_{i=1}^{3} g_i \boldsymbol{e}_i^{\perp}$ are conventional and generalized body force densities. The differential operators $\partial_i = \partial/\partial x_i$ $(i = 1, 2, 3)$ and $\boldsymbol{\nabla} = \sum_{i=1}^{3} \boldsymbol{e}_i \partial_i$ are relative to the position vector $\boldsymbol{r} = \sum_{i=1}^{3} \boldsymbol{e}_i x_i \in E^{\parallel}$ only. It should be emphasized that both $\boldsymbol{u}$ and $\boldsymbol{w}$ only depend on the position vector $\boldsymbol{r}$ in the parallel space $E^{\parallel}$.

Equation (1) is too complicated to solve in analytical form. In view of this, firstly, we consider only the case in which the body force densities $\boldsymbol{f}$ and $\boldsymbol{g}$ can be omitted. Secondly, we decouple $\boldsymbol{u}$ and $\boldsymbol{w}$ by letting $R = 0$, which has been used in the atomic modelling of dislocations in Al–Pd–Mn IQCs [8]. Thirdly, we assume $K_2 = 0$, which was proposed by Bachteler *et al* [25] as the so-called 'spherical approximation'. Under these assumptions the basic equation (1) is reduced to

$$\begin{aligned}
&\mu\nabla^2 u_1 + (\lambda+\mu)\partial_1(\boldsymbol{\nabla}\cdot\boldsymbol{u}) = 0,\\
&\mu\nabla^2 u_2 + (\lambda+\mu)\partial_2(\boldsymbol{\nabla}\cdot\boldsymbol{u}) = 0,\\
&\mu\nabla^2 u_3 + (\lambda+\mu)\partial_3(\boldsymbol{\nabla}\cdot\boldsymbol{u}) = 0,\\
&K_1\nabla^2 w_1 = 0,\\
&K_1\nabla^2 w_2 = 0,\\
&K_1\nabla^2 w_3 = 0.
\end{aligned} \tag{2}$$

It can be written in vector form as

$$\begin{aligned}
&\mu\nabla^2\boldsymbol{u} + (\lambda+\mu)\boldsymbol{\nabla}(\boldsymbol{\nabla}\cdot\boldsymbol{u}) = 0,\\
&K_1\nabla^2\boldsymbol{w} = 0.
\end{aligned} \tag{3}$$

It must be emphasized that IQCs, the quasicrystals of highest symmetry, are not elastically isotropic. It is only when the elastic constants $R = K_2 = 0$, as supposed in equations (2) and (3), that an IQC behaves like an isotropic medium.

It is convenient to discuss the displacement field induced by a spherical inclusion in a spherical coordinate system. For a spherical inclusion, the displacement fields $\boldsymbol{u}$ and $\boldsymbol{w}$, which fulfil equations (2) and (3), are only functions of the radial component r in the spherical coordinate system, independent of θ and ϕ. Furthermore, $\boldsymbol{u} = u(r)\boldsymbol{r}_0$ has only a radial component, while $\boldsymbol{w} = w(r)\boldsymbol{w}_0$ possesses an invariant direction $\boldsymbol{w}_0$, which is independent of $\boldsymbol{r}$, and a variable modulus $w(r)$, which is a function of r. Thus equation (3) can be reduced in the spherical coordinate system as follows (the details of the derivation are given in the appendix):

$$\begin{aligned}
&\frac{\mathrm{d}}{\mathrm{d}r}\left(\frac{\mathrm{d}u}{\mathrm{d}r} + \frac{2u}{r}\right) = 0,\\
&\frac{\mathrm{d}}{\mathrm{d}r}\left(r^2\frac{\mathrm{d}w}{\mathrm{d}r}\right) = 0.
\end{aligned} \tag{4}$$

The general solutions of the differential equations (4) have the following forms:

$$\begin{aligned}
&u(r) = Ar + Br^{-2},\\
&w(r) = C + Dr^{-1}.
\end{aligned} \tag{5}$$

In order to obtain the concrete analytical expressions for u and w we should give boundary conditions. For a spherical defect of radius of r_0 in an IQC, these conditions can be: $r \to 0$, u and w are finite; $r \to \infty$, $u = 0$, $w = 0$; u and w are continuous at $r = r_0$, thus we have

$$u = \begin{cases} \epsilon_1 r & (r \leqslant r_0), \\ \epsilon_1 r_0^3 r^{-2} & (r \geqslant r_0), \end{cases} \tag{6a}$$

$$w = \begin{cases} \epsilon_2 & (r \leqslant r_0), \\ \epsilon_2 r_0 r^{-1} & (r \geqslant r_0), \end{cases} \tag{6b}$$

where ϵ_1 is a constant related to the elastic constants and the misfit between the spherical particle (P) and matrix (M), and $\epsilon_2 \boldsymbol{w}_0$ is a constant vector in perpendicular subspace describing a phason-type shift of the spherical defect relative to the matrix.

The expression for ϵ_1 may be obtained as follows: if $\delta = (a_\mathrm{P} - a_\mathrm{M})/[(a_\mathrm{P} + a_\mathrm{M})/2]$ is the misfit between the spherical particle and matrix, the particle undergoes a homogeneous strain of $\epsilon_1 - \delta$ and a pressure of $3(\epsilon_1 - \delta)K_\mathrm{P}$, where K_P is the bulk modulus of the particle. On the other hand, the radial strain in the matrix is $\mathrm{d}u/\mathrm{d}r = -2\epsilon_1 r_0^3/r^3$ which corresponds to a radial stress of $-4\mu_\mathrm{M}\epsilon_1$ at the boundary ($r = r_0$), where μ_M is the shear modulus of the matrix. The elastic equilibrium between the particle and matrix requires continuity of the stress at the boundary: $3(\epsilon_1 - \delta)K_\mathrm{P} = -4\mu_\mathrm{M}\epsilon_1$, which leads to the following expression for the constant ϵ_1:

$$\epsilon_1 = \frac{3K_\mathrm{P}\delta}{3K_\mathrm{P} + 4\mu_\mathrm{M}}. \tag{7}$$

3. Applications of expressions (6) to the simulations of x-ray topography (XRT) images

3.1. Three concrete cases

The analytical expression derived here (equations (6)) for the phonon-type component u is the same as that for a spherical inclusion in conventional elastically isotropic crystals [10], while the expression for the phason-type displacement w, which decreases with increasing distance r to the sphere centre as r^{-1}, is derived for the first time. These results are useful for studying the strain field around spherical inclusions in IQCs, such as pores (holes), bubbles, inclusion phases, antiphase domains. There are three cases to be considered:

(1) $w = 0$, but $u \neq 0$. If a spherical inclusion is a hole (pore), or a bubble, or a crystalline precipitate, where no phason-type displacement relative to the matrix exists ($\epsilon_2 \boldsymbol{w}_0 = 0$), there would be no phason-type displacement field in the IQC matrix around these inclusions, according to the continuity of the phason-type displacement at the boundary of the defect.

Obviously this consideration is only a first-order approximation when the phonon–phason coupling effect is neglected and the matrix is only deformed elastically around the inclusion without any plastic deformation carried out by dislocation gliding.

(2) $u = 0$, but $w \neq 0$. If the spherical inclusion is an IQC which possesses the same structure and composition as the matrix, but is a local isomorphism with a non-zero phason-type displacement $\epsilon_2 \boldsymbol{w}_0$ relative to the IQC matrix, there will be a phason-type displacement field but no phonon-type displacement field around the inclusion, because the misfit δ between the spherical particle and matrix is equal to zero. The inclusion will be bounded by a peculiar antiphase boundary which could be considered as a peculiar class of structural defects in IQCs.

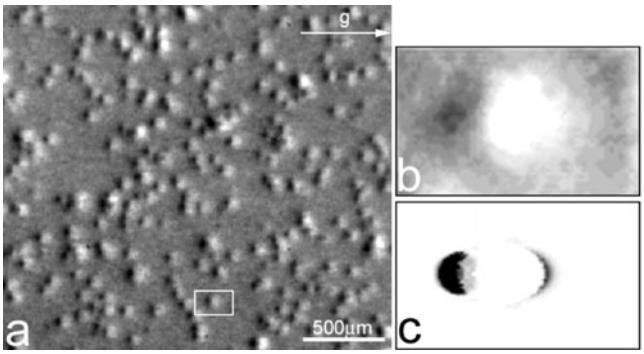

Figure 1. (a) An experimental XRT image of the black–white double-lobe contrasts; (b) one enlarged image of the black–white double-lobe contrast; (c) the corresponding simulated XRT image.

(3) $u \neq 0$, $w \neq 0$. If the spherical inclusion is an IQC which possesses different structure and/or composition compared with the matrix, and is a local isomorphism with a non-zero phason-type displacement $\epsilon_2 \boldsymbol{w}_0$ relative to the IQC matrix, there will be both phonon- and phason-type displacement fields around the inclusion.

3.2. Application of expression (6a): black–white double-lobe contrasts

In experiments, pores [11–21, 23] are a common type of inhomogeneity, observed in various quasicrystals, in addition to structural defects such as dislocations, small dislocation loops, stacking faults. Audier *et al* [11] observed faceted holes of dodecahedral shape to develop within the IQC phase by transmission electron microscopy when thin fragments of Al–Cu–Fe alloys were annealed within the microscope. Beeli *et al* [12] found faceted micro-holes in slowly cooled icosahedral single Al–Mn–Pd quasicrystals by scanning electron microscopy (SEM). Gödecke and Lück [13] reported their SEM observation of polyhedral etch pits, showing pentagons or decagons and triangles as facets, in Al–Pd–Mn IQCs. Waseda *et al* [14, 15] analysed the dodecahedral voids in single-quasicrystalline Al–Pd–Mn IQCs by SEM and Auger electron spectroscopy. Ross *et al* [16] observed the formation and morphological development of porosity (unfaceted and faceted) in Al–Pd–Mn IQCs.

Recently, Mancini *et al* [17] demonstrated by phase-sensitive radiography (PSR) that the dodecahedral pores are also located in the bulk of Al–Pd–Mn IQCs. Besides this technique, this group also exploited x-ray topography (XRT) to observe the strain field around the pores and their evolution during annealing [17–21, 23]. By combining these two techniques, a correspondence was found between the black–white double-lobe contrasts shown in figure 1(a), observed by XRT, and the dodecahedral pores observed by PSR. Above that, the black–white double-lobe contrasts in XRT images were simulated, using a 3D displacement field calculated by u in expression (6a). The simulation was carried out by using the program TOPLANE [26] in the monochromatic case. One simulated image is shown here in figure 1(c), which shows good agreement with the corresponding experimental one, shown in figure 1(b). This is just case (1) discussed in section 3.1.

3.3. Application of expression (6b): loop-shaped contrasts (LSCs)

Besides the black–white double-lobe contrasts induced by pores, Gastaldi and his colleagues [17–19, 21–24] observed other novel loop-shaped contrasts (LSCs) in Al–Pd–Mn

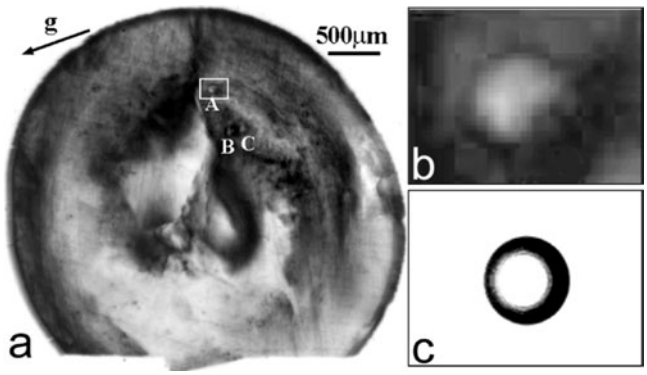

Figure 2. (a) An experimental XRT image of the LSCs; (b) an enlarged XRT image of a LSC; (c) the corresponding simulated XRT image when $\boldsymbol{G}^{\perp} \cdot \boldsymbol{B}^{\perp} \neq 0$ is adopted.

and Al–Cu–Fe IQCs by XRT and no correspondence was found between the LSCs and the pores by PSR. Hence these LSCs were not caused by the strain field around pores.

Further preliminary experimental observations were performed on the LSCs.

(1) We observed LSCs in as-grown $Al_{70.3}Pd_{20.6}Mn_{9.1}$ IQC by means of traditional XRT (Lang's technique). Various diffraction vectors were excited to record XRT images [22], of which one is shown in figure 2(a). Detailed analysis of the extinction phenomena as listed in [22] reveals that the extinction is due to $\boldsymbol{G}^{\perp} \cdot \boldsymbol{B}^{\perp} = 0$, with $\boldsymbol{B} = [1\bar{1}0\bar{1}01]$.
(2) The LSCs cannot be ascribed to dislocation loops due to annealing behaviour different from that for dislocations [19].
(3) The same diffracted intensity for the inner and outer parts of the LSCs indicates that the atomic structures of these two parts are almost the same [24].
(4) The intensity of the LSCs becomes weaker on using reflections of smaller perpendicular components $\boldsymbol{G}^{\perp}$ in the XRT experiment [24].

All these experimental observations prompt us to explain the LSC as caused by a strain field around a novel, peculiar class of antiphase domain, of which the interior is a local isomorphism with a non-zero phason-type displacement $\epsilon_2 \boldsymbol{w}_0$ (i.e. $\boldsymbol{B}^{\perp}$) relative to the IQC matrix, as discussed in case (2) of section 3.1.

Thus the displacement field w in equations (6*b*) of the present letter was used to simulate the LSC XRT image also by using the TOPLANE program [26]. When $\boldsymbol{G}^{\perp} \cdot \boldsymbol{B}^{\perp} \neq 0$ was used, we got the LSC in the simulated XRT image as shown in figure 2(c). The agreement between the experimental (figure 2(b)) and the simulated (figure 2(c)) XRT images supports this explanation of the LSCs.

4. Conclusions

In this letter, we obtain the analytical expressions as a first-order approximation for the elastic displacement fields, including both phonon- and phason-type components, induced by spherical inclusions in IQCs. Three concrete cases are discussed. Then, the phonon part of the analytical expressions was used to simulate the black–white double-lobe contrasts in the XRT images of the strain field around the pores in the AlPdMn IQCs. The analytical expression for the phason-type displacement is used to simulate the LSCs of the strain field around spherical inclusions having isomorphic structures. The striking resemblance between

experimental and simulated images suggests that such inclusions are surrounded by antiphase boundaries with a phason-type displacement vector, being particular structural defects in IQCs.

This work was partially supported by the Scientific Research Foundation for the Returned Overseas Chinese Scholars, State Education Ministry, the National Natural Science Foundation of China (Grant No 19974030), the Research Fund for the Doctoral Programme of Higher Education of China, and the Chinese–French Cooperative Project (4C5-007). The authors are grateful to Professors Di-Hua Ding and Chengzheng Hu, and Drs J Härtwig, H Klein and S Agliozzo for useful discussions, and to Professor Y Epelboin for providing the TOPLANE program and discussions on simulation.

Appendix. Derivation of the elastic equations (4)

Notice that the unit vectors $\boldsymbol{r}_0$, $\boldsymbol{\theta}_0$ and $\boldsymbol{\phi}_0$ in the spherical system are not constant but vary with the coordinates r, θ and ϕ; we have

$$\boldsymbol{\nabla}\boldsymbol{u} = \boldsymbol{\nabla}(u\boldsymbol{r}_0) = \boldsymbol{r}_0\frac{\mathrm{d}u}{\mathrm{d}r}\boldsymbol{r}_0 + \boldsymbol{\theta}_0\frac{u}{r}\boldsymbol{\theta}_0 + \boldsymbol{\phi}_0\frac{u}{r}\boldsymbol{\phi}_0,$$

$$\boldsymbol{\nabla}\cdot\left(\boldsymbol{r}_0\frac{\mathrm{d}u}{\mathrm{d}r}\boldsymbol{r}_0\right) = \frac{\boldsymbol{r}_0}{r^2}\frac{\mathrm{d}}{\mathrm{d}r}\left(r^2\frac{\mathrm{d}u}{\mathrm{d}r}\right),$$

$$\boldsymbol{\nabla}\cdot\left(\boldsymbol{\theta}_0\frac{u}{r}\boldsymbol{\theta}_0\right) = -\boldsymbol{r}_0\frac{u}{r^2} + \boldsymbol{\theta}_0\frac{u}{r^2}\cot\theta,$$

$$\boldsymbol{\nabla}\cdot\left(\boldsymbol{\phi}_0\frac{u}{r}\boldsymbol{\phi}_0\right) = -\boldsymbol{r}_0\frac{u}{r^2} - \boldsymbol{\theta}_0\frac{u}{r^2}\cot\theta.$$

Hence we have

$$\nabla^2\boldsymbol{u} = \nabla^2(u\boldsymbol{r}_0) = \boldsymbol{r}_0\frac{\mathrm{d}}{\mathrm{d}r}\left(\frac{\mathrm{d}u}{\mathrm{d}r} + \frac{2u}{r}\right).$$

Moreover, we have

$$\boldsymbol{\nabla}(\boldsymbol{\nabla}\cdot\boldsymbol{u}) = \boldsymbol{\nabla}[\boldsymbol{\nabla}\cdot(u\boldsymbol{r}_0)] = \boldsymbol{\nabla}\left[\frac{1}{r^2}\frac{\mathrm{d}}{\mathrm{d}r}(r^2u)\right] = \boldsymbol{r}_0\frac{\mathrm{d}}{\mathrm{d}r}\left(\frac{\mathrm{d}u}{\mathrm{d}r} + \frac{2u}{r}\right).$$

Hence the equation

$$\mu\nabla^2\boldsymbol{u} + (\lambda+\mu)\boldsymbol{\nabla}(\boldsymbol{\nabla}\cdot\boldsymbol{u}) = (\lambda+2\mu)\boldsymbol{r}_0\frac{\mathrm{d}}{\mathrm{d}r}\left(\frac{\mathrm{d}u}{\mathrm{d}r} + \frac{2u}{r}\right) = 0$$

is reduced to the first of equations (4).

Since the unit vector $\boldsymbol{w}_0$ in $\boldsymbol{w} = w\boldsymbol{w}_0$ is a constant vector in the perpendicular subspace, which indicates that $\boldsymbol{w}_0$ is independent of $\boldsymbol{r}$, and w is a function of only r,

$$\nabla^2\boldsymbol{w} = \nabla^2(w\boldsymbol{w}_0) = \frac{\boldsymbol{w}_0}{r^2}\frac{\mathrm{d}}{\mathrm{d}r}\left(r^2\frac{\mathrm{d}w}{\mathrm{d}r}\right) = 0.$$

Hence the equation $\nabla^2(w\boldsymbol{w}_0) = 0$ leads to $\frac{\mathrm{d}}{\mathrm{d}r}\left(r^2\frac{\mathrm{d}w}{\mathrm{d}r}\right) = 0$, which is the second of equations (4).

References

[1] Stadnik Z (ed) 1999 *Physical Properties of Quasicrystals (Springer Series in Solid State Sciences vol 126)* (Berlin: Springer)
[2] Levine D and Steinhardt P 1986 *Phys. Rev.* B **34** 596
[3] Socolar J and Steinhardt P 1986 *Phys. Rev.* B **34** 617
[4] Edagawa K, Suzuki K and Takeuchi S 2000 *Phys. Rev. Lett.* **85** 1674

[5] Ding D-H, Yang W, Hu C and Wang R 1993 *Phys. Rev.* B **48** 7003
[6] Ding D-H, Wang R, Yang W and Hu C 1998 *Prog. Phys.* **18** 223 (in Chinese)
[7] Hu C, Wang R and Ding D-H 2000 *Rep. Prog. Phys.* **63** 1
[8] Yang W, Feuerbacher M, Tamura N, Ding D-H, Wang R and Urban K 1998 *Phil. Mag.* A **77** 1481
[9] Wang J and Qin Y 2002 *Phys. Rev.* B **65** 026201
[10] Mott N and Nabarro F 1940 *Proc. Phys. Soc.* **52** 86
[11] Audier M, Guyot P and Brechet Y 1990 *Phil. Mag. Lett.* **61** 55
[12] Beeli C and Nissen H-U 1993 *Phil. Mag.* B **68** 487
[13] Gödecke T and Lück R 1995 *Z. Metallk.* **86** 109
[14] Suzuki S, Waseda Y and Urban K 1998 *Mater. Trans. JIM* **39** 314
[15] Waseda Y, Suzuki S and Urban K 1998 *Z. Naturf.* a **53** 679
[16] Ross A, Wiener T, Fisher I, Canfield P and Lograsso T 2000 *Mater. Sci. Eng.* A **294–296** 53
[17] Mancini L, Reinier E, Cloetens P, Gastaldi J, Härtwig J, Schlenker M and Baruchel J 1998 *Phil. Mag.* A **78** 1175
[18] Gastaldi J, Reinier E, Jourdan C, Grange G, Quivy A and Boudard M 1995 *Phil. Mag. Lett.* **72** 311
[19] Reinier E, Mancini L, Gastaldi J, Baluc N, Härtwig J and Baruchel J 1998 *Physica* B **253** 61
[20] Mancini L, Janot C, Loreto L, Farinato R, Gastaldi J and Baruchel J 1998 *Phil. Mag. Lett.* **78** 159
[21] Mancini L, Létoublon A, Agliozzo S, Wang J, Gastaldi J, de Boissieu M, Härtwig J and Klein H 2000 *Mater. Sci. Eng.* A **294–296** 57
[22] Wang J, Gastaldi J and Wang R 2001 *Chin. Phys. Lett.* **18** 88
[23] Mancini L 1998 *PhD Thesis* Université Joseph Fourier–Grenoble I, Grenoble, France
[24] Klein H, Agliozzo S, Mancini L, Gastaldi J, Härtwig J and Baruchel J 2001 *J. Phys. D: Appl. Phys.* **34** A98
[25] Bachteler J and Trebin H-R 1998 *Eur. Phys. J.* B **4** 299
[26] Epelboin Y 1999 *TOPLANE, TOPRC: Simulation of Plane Wave Topographs and Rocking Curve Profiles in the Laue Case (User's Guide, Version 2.0)*